Complex Formation by Electrostatic Interaction between Carboxyl-Terminated Dendrimers and Oppositely Charged Polyelectrolytes†

Nobuhiro Miura,‡ Paul L. Dubin,* C. N. Moorefield,§ and G. R. Newkome§

Department of Chemistry, Indiana University−Purdue University, Indianapolis, Indianapolis, Indiana 46202

Received February 8, 1999. In Final Form: March 22, 1999

Complex formation between a carboxyl-terminated cascade polymer (generation 3) and several cationic polyelectrolytes of varying linear charge density was studied as a function of ionic strength, by turbidimetric titration and dynamic light scattering. Tetramethylammonium chloride was used to adjust the ionic strength in order to avoid sodium counterion binding to dendrimer carboxyl groups. Complex formation occurred abruptly at a critical pH, as signaled by a sudden change in either the turbidity or the apparent Stokes radius from dynamic light scattering. The pH_c of incipient complex formation was converted to the critical surface charge density σ_c. Under conditions of low or moderate ionic strength (I), it was confirmed that σ_c is roughly proportional to κ/ξ, where $\kappa \sim I^{1/2}$ is the Debye−Hückel parameter and ξ is the linear charge density of the polyelectrolyte.

Introduction

Intermacroionic complex formation is a basic phenomenon in biological systems[1] as well as in a number of technological processes;[2] however, in the case of biological systems such as protein−DNA and enzyme−substrate complexes, the mechanism of intermolecular interaction is difficult to fully elucidate in physicochemical terms. For example, ligand binding constants, related to biological activity, cannot be quantitatively explained solely on the basis of fundamental variables such as macromolecular charge density or the electrostatic screening effect of the counterion. For such reasons, and also because of the technological relevance of colloid−polymer interactions, we focus on complex formation arising from electrostatic interactions in synthetic systems of polyelectrolytes and oppositely charged colloid particles. The colloidal particle in this study is a symmetric, uniform, and spherical dendrimer[3] which provides an ideal model for small charged colloids.

The binding of polyelectrolytes and oppositely charged particles depends predominantly on three variables: the ionic strength (I), the polymer linear charge density (ξ), and the colloid surface charge density (σ). Phase-transition-like behavior for the interaction of polyelectrolytes with oppositely charged particles has been predicted by several theoretical investigations.[4−8] Previous experimental studies on micelle−,[9−12] dendrimer−,[13,14] and protein−polyelectrolyte[15−17] systems have revealed the existence of such critical conditions for complexation. Studies with polyelectrolytes and oppositely charged micelles have suggested the empirical relationship

$$\sigma_c \xi \sim \kappa \tag{1}$$

where κ is the Debye−Hückel parameter ($\kappa \sim I^{1/2}$) and σ_c is the critical surface charge density of the micelle at the point of incipient complex formation.[9] In the case of a dendrimer−polyelectrolyte system, it was observed that σ_c depends on the ionic strength,[13,14] but the relationship among σ_c, ξ, and κ was not confirmed.

In this report, we examine the dependence of σ_c on ξ and κ. The quantity ξ is varied by using copolymers of ((methacrylamido)propyl)trimethylammonium chloride (MAPTAC) and acrylamide (AAm). Sodium counterion binding to carboxyl-terminated dendrimer has been demonstrated by potentiometric titration,[18] so it may be expected to affect complexation; therefore, both TMACl and NaCl were used to adjust the ionic strength (I). The mechanism of phase separation is also briefly discussed in this study, since observations of phase separation by complexation may help us to understand the mechanism

† Presented at Polyelectrolytes '98, Inuyama, Japan, May 31−June 3, 1998.

‡ Current address: Polymer Science & Engineering, University of Massachusetts, Amherst, MA 01002.

§ Department of Chemistry, University of South Florida, Tampa, FL 33620.

(1) Lilley, D. M. J. *DNA−Protein: Structural Interactions*; IRL Press: Oxford, U.K., 1995; pp 26−27.
(2) Evans, D. F.; Wennerstrom, H. *The Colloidal Domain: Where Physics, Chemistry, Biology, and Technology Meet*; VCH Publishers: New York, 1994; pp 455−496.
(3) Newkome, G. R.; Moorefield, C. N.; Vögtle, F. *Dendritic Molecules: Concepts, Syntheses, Perspectives*; VCH: Weinheim, Germany, 1996.
(4) Odijk, T. *Langmuir* **1991**, *7*, 1991.
(5) von Goeler, F.; Muthukumar, M. *J. Chem. Phys.* **1994**, *100*, 7796.
(6) Wiegel, F. W. *J. Phys. A: Math. Gen.* **1977**, *10*, 299.
(7) Varoqui, R.; Johner A.; Elaissari, A. *J. Chem. Phys.* **1991**, *94*, 6874.
(8) Evers, O. A.; Fleer, G. J.; Scheutjens, J. M. H. M.; Lyklema, J. *J. Colloid Interface Sci.* **1986**, *111*, 446.
(9) McQuigg, D. W.; Kaplan, J. I.; Dubin, L. P. *J. Phys. Chem.* **1992**, *96*, 1973.
(10) Li, Y.; Xia, J.; Dubin, P. L. *Macromolecules* **1994**, *27*, 7049.
(11) Li, Y.; Dubin, L. P.; Dautzenberg, H.; Luck, U.; Hartmann, J.; Tuzar, Z. *Macromolecules* **1995**, *28*, 6795.
(12) Yoshida, K.; Sokhakian, S.; Dubin, P. L. *Colloids Surf.*, in press.
(13) Li, Y.; Dubin, P. L.; Spindler, R.; Tomalia, D. A. *Macromolecules* **1995**, *28*, 8426.
(14) Zhang, H.; Dubin, P. L.; Spindler, R.; Tomalia, D. A. *Ber. Bunsen-Ges. Phys. Chem.* **1996**, *100*, 923.
(15) Li, Y.; Mattison, K. W.; Dubin, P. L.; Havel, H. A.; Edwards, S. L. *Biopolymers* **1996**, *38*, 527.
(16) Xia, J.; Mattison, K.; Romano, V.; Muhoberac, B. B. *Biopolymers* **1997**, *41*, 359.
(17) Mattison, K. W.; Dubin, P. L.; Brittain, I. J. *J. Phys. Chem. B* **1998**, *102*, 3830.
(18) Zhang, H.; Dubin, P. L.; Kaplan, J.; Moorefield, C. N.; Newkome, G. R. *J. Phys. Chem.* **1997**, *101*, 3495.

10.1021/la990125l CCC: $18.00
Published on Web 05/13/1999

of precipitation and complex coacervation (liquid−liquid polyelectrolyte phase separation) in general.

Experimental Section

Materials. The third-generation cascade methane[4]−(3-oxo-6-oxa-2-azaheptylidyne)−(3-oxo-2-azapentylidyne)^2−propanoic acid (G3) has 108 terminal COOH groups and a theoretical molecular weight of 12 345.[19,20]

Poly(diallyldimethylammonium chloride) (PDADMAC), molecular weight 458 000, was synthesized by free-radical polymerization of diallyldimethylammonium chloride, purified, and characterized in the laboratory of Dr. W. Jaeger (Fraunhofer-Institut, Teltow, Germany). Poly[(methacrylamido)propyl)trimethylammonium chloride] (PMAPTAC) was a gift from Clairol corporation, Stamford, CT. Copolymers of MAPTAC and acrylamide (AAm), 60, 40, and 30% MAPTAC, were prepared by Dr. Takeshi Sato at Osaka University. A 15% MAPTAC and AAm copolymer was from Jefferson Chemical Company, Inc., Bellaire, Texas. Studies with micelle-polyelectrolyte or protein−polyelectrolyte systems have shown that polymer MW has no effect on σ_c,[10,11] so no attempt was made to characterize MW for these copolymers. The average linear polymer charge density ξ was obtained as the reciprocal of contour length charge spacing: 2.5 Å for PMAPTAC, 6.2 Å for PDADMAC, 3.1 Å for MAPTAC−AAm (80:20), 4.2 Å for MAPTAC−AAm (60:40), 6.3 Å for MAPTAC−AAm (40:60), and 16.7 Å for MAPTAC−AAm (15:85).

Sodium chloride (NaCl) and tetramethylammonium chloride (TMACl) were purchased from Sigma and Aldrich Chemical Co. Inc., respectively. NaOH, HCl, and buffer solutions of pH 4.00 ± 0.01 and pH 7.00 ± 0.01 were from Fisher Scientific.

Potentiometric Titration. Potentiometric titrations with 0.5 M HCl or 0.5 M NaOH were performed with an Orion pH meter 811 at 23 ± 1 °C. The pH meter was calibrated with 4.00 ± 0.01 and 7.00 ± 0.01 buffers just before titration. The instrumental drift was less than 0.02 during titration. Nitrogen gas was bubbled through the solution to remove carbon dioxide in the solution for 10 min before the titration, and the solution was then maintained under N_2. A 2.0 mL microburet was used to add 0.500 M NaOH or 0.500 M HCl to a 10.00 mL aqueous solution of dendrimer (0.50 g/L), containing the desired concentration of NaCl or TMACl and with initial pH adjusted to 7.00 ± 0.03. These titrations were always accompanied by a blank titration of dendrimer-free solution. The amount of acid or base contributed to the neutralization reaction was estimated as the difference, ΔV, in added HCl or NaOH between dendrimer solution and blank solution at the same pH. Successful blank correction was indicated by the appearance of asymptotic end points corresponding to degrees of dissociation $\alpha = 0$ and 1 in the ΔV versus pH plots (see Figure 1). α was determined as

$$\alpha = (\Delta V - \Delta V_0)/\Delta V_T = [COO^-]/([COOH] + [COO^-]) \quad (2)$$

where ΔV_T is the total value between $\alpha = 0$ and 1, and ΔV_0 is ΔV at $\alpha = 0$. Sample plots of pH against the α value of the dendrimer in 0.1 M TMACl and NaCl are shown in Figure 2.

Turbidimetric Titration. The pH dependence of turbidity was measured using a Brinkman PC 800 colorimeter equipped with a 1 cm path length optical probe, at 23 ± 1 °C. The colorimeter was calibrated to read 100% transmittance with Milli-Q water. The solutions (0.10 g/L) were filtered with 0.2 μm Whatman filters before turbidimetric titration. All titrations were carried out with magnetic stirring, and the time interval between measurements was about 1 min. After mixing, solutions with transmittances corresponding to 100 − %T < 5 were always stable with respect to both turbidity and DLS measurements.

Dynamic Light Scattering. Dynamic light scattering (DLS) measurements were performed using a DynaPro-801 (Protein Solutions Inc., Charlottesville, VA), equipped with a 780 nm solid-state laser of approximately 25 mW power and an avalanche photodiode detector. All solutions were filtered with 0.2 μm Whatman filters before DLS measurement. The intensity−intensity autocorrelation function $G^{(2)}(\tau)$, which expresses the temporal fluctuation of the intensity of scattered light, is obtained from measured light scattering by

$$G^{(2)}(\tau) = \sum I(t_j)\, I(t_j - \tau) \quad (3)$$

where $I(t)$ is the scattering intensity at time t and τ is the delay time. The autocorrelation function was analyzed via CONTIN. The decay constant τ_0 was determined by fitting of $G^{(2)}(\tau)$ to the function

$$G^{(2)}(\tau) = B + C \exp(\tau/\tau_0) \quad (4)$$

where B is the baseline and C is the gain of the decay function. Assuming that the particle is uniform and that interparticle interactions are negligible, the translational diffusion coefficient of the molecule D_T was estimated by

$$D_T = q^2/\tau_0 \quad (5)$$

in which $q = (4\pi n/\lambda_0)\sin(\theta/2)$ is the magnitude of the scattering vector, n is the refractive index of the solution, θ is the scattering angle, and λ_0 is the wavelength of light in a vacuum. Then the z-average apparent hydrodynamic radius R_S^{app} of the particles was derived from D_T using the Stokes−Einstein equation:

$$D_T = kT/6\pi\eta R_S^{app} \quad (6)$$

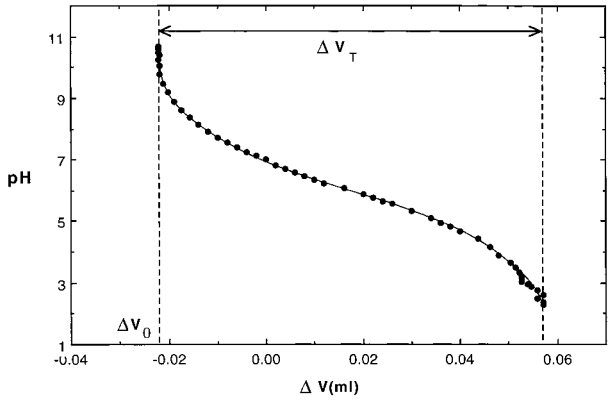

Figure 1. Titration of dendrimer G3 in 0.1 M TMACl presented as blank-corrected titrant volume versus pH. Negative values of ΔV correspond to titration with 0.500 M NaOH, and positive values to titration with 0.500 M HCl. ΔV_T is the total value between $\alpha = 0$ and $\alpha = 1$, and ΔV_0 is ΔV at $\alpha = 0$.

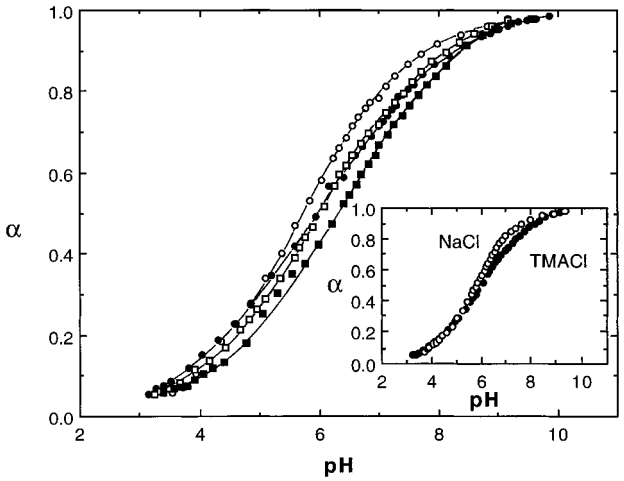

Figure 2. G3 titration curves in TMACl: 0.050 M (■); 0.100 M (□); 0.200 M (●) 0.500 M (○); obtained from data as in Figure 1. Inset: G3 titration curves in 0.1 M TMACl (▲) and NaCl (○).

(19) Newkome, G. R.; Young, J. K.; Baker, G. R.; Potter, R. L.; Audoly, L.; Cooper, D.; Weis, C. D. *Macromolecules* **1993**, *26*, 2394.

(20) Young, J. K.; Baker, G. R.; Newkome, G. R.; Morris, K. F.; Johnson, C. S., Jr. *Macromolecules* **1994**, *27*, 3464.

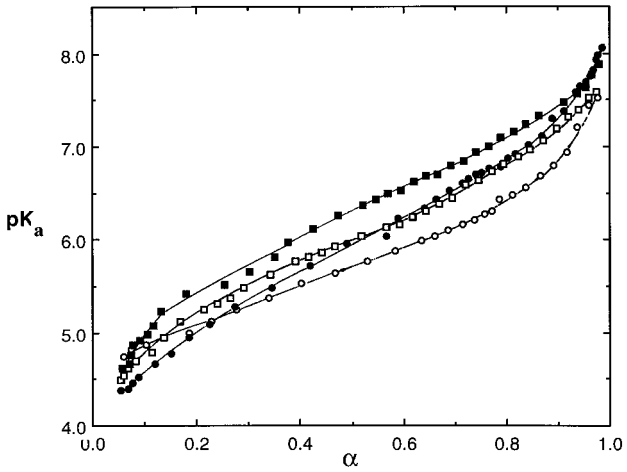

Figure 3. pK_a versus α for G3 in TMACl: 0.050 M (■); 0.100 M (□); 0.200 M (●) 0.500 M (○).

where k is the Boltzmann constant, T is the absolute temperature, and η is the solvent viscosity. Our interest is only the determination of the pH at which R_S^{app} changes abruptly, so its absolute value is not of primary concern.

Results and Discussion

Potentiometric Titration. The relationship between pH and α for dendrimer G3 in 0.1 M TMACl and NaCl is shown in Figure 2. The results in TMACl and NaCl converge below pH 5, but the slope in NaCl is steeper than that in TMACl in the region between pH 5 and pH 7. This result suggests that the binding of Na^+ to dendrimer increases the acidity of the carboxylic acid groups, an effect not seen for the nonbinding TMA^+. The tendency of Na^+ to bind to carboxylate has been well-documented.[21] To avoid counterion binding, TMACl was therefore used to control ionic strength in addition to NaCl.

Dendrimer solutions of 0.5 g/L at various ionic strengths of TMACl were titrated with 0.500 ± 0.002 M HCl and NaOH. Titration curves of G3 in various TMACl concentrations are shown in Figure 3 as the α-dependence of the apparent pK, p$K_a \equiv$ pH + log(1 − α)/α.

Phase Separation and Complexation between Dendrimer G3 and Polyelectrolyte. Turbidimetric titrations for dendrimer G3 in the presence of MAPTAC−AAm (40%/60%) copolymer in TMACl at various ionic strengths are shown in Figure 4A. The sudden increase in turbidity at a well-defined pH_c arises because phase separation is a result of complexation. The increase in pH_c with ionic strength is due to screening. The behavior of PDADMAC−G3 in NaCl in Figure 4B is more complicated and will be discussed below. All the results are summarized in Tables 1 and 2 and plotted as pH_c versus I in Figure 5. Since it is difficult to estimate α_c in the low-pH region, most of the data in Figure 5 are for the low-charge-density polyelectrolyte, and there is only one data point for PMAPTAC.

The pH dependence of the apparent hydrodynamic radius R_S^{app} for G3/PDADMAC in 0.50 M NaCl and for G3/MAPTAC−AAm (15%/85%) in 0.10 M NaCl is shown in Figure 6. For the copolymer, the discontinuity in R_S^{app} corresponds to the pH_c determined by turbidimetric titration and confirms the use of the latter method for determining pH_c. However, in the case of PDADMAC, R_S^{app} changes gradually, and the discontinuity is not clear and does not agree with the pH_c determined by turbidimetric titration.

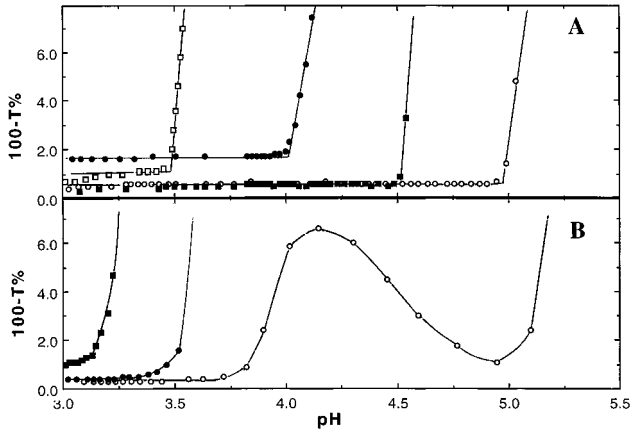

Figure 4. (A) Turbidity (100 − %T) versus pH for dendrimer G3 + PMAPTAC−AAm (40%/60%) at the ionic strengths (TMACl) 0.100 M (□), 0.200 M (●), 0.300 M (■), and 0.400 M (○). (B) Turbidity (100 − %T) versus pH for dendrimer G3 + PDADMAC at the ionic strengths (NaCl) 0.200 M (■), 0.350 M (●) and 0.500 M (○).

The effects of NaCl versus TMACl may also be seen for dendrimer G3/MAPTAC−AAm (60/40) from the plots of pH_c versus I in Figure 5 (open and filled triangles). The critical pH in TMACl is smaller than that in NaCl, this tendency increasing with increasing ionic strength. These results suggest that Na^+ binding to dendrimer interferes with its binding to polyelectrolyte and thus impedes complexation and phase separation. As seen in Figure 4B for PDADMAC in NaCl, pH_c is separated from pH_ϕ, corresponding to the formation of a soluble complex without phase separation. The maximum in turbidity for PDADMAC in 0.50 M NaCl as a function of pH may in fact correspond to the formation of soluble complexes, followed by their redissolution at high pH due to charge reversal. Evidence of soluble complex formation may be discerned also for the other homopolymer, PMAPTAC, as seen in Figure 7. The "steps" between pH_c and pH_ϕ in Figure 7 result from the instrumental limit of ±0.1%T; however, the instrumental drift of the system is less than 0.1 per 1 h, so the subtle increase in turbidity from pH 3.5 to pH 4.1 is real.

The pH dependence of R_S^{app} for PDADMAC in Figure 6 indicates the presence of soluble complexes before phase separation. Such soluble complexes were also observed in protein−polyelectrolyte and micelle−polyelectrolyte systems. Since phase separation is likely to occur by charge neutralization,[22] soluble complexes presumably bear some excess charge. The situation is represented schematically in Figure 8. When complex formation occurs at low α, the bound dendrimer charge cannot cancel the highly charged polyelectrolyte and excess charge arises. Thus, soluble complex is observed in systems showing low pH_c.

Although the linear charge density ξ of PDADMAC is nearly the same as that of the 40% MAPTAC copolymer, its pH_c is lower. This shift of pH_c is too large to explain by the difference between Na^+ and TMA^+, since the effect of counterion binding is small at low ionic strength. Similar anomalous behavior has been observed in protein−polyelectrolyte systems (e.g. bovine serum albumin with PDADMAC versus a 50/50 copolymer of trimethylaminoethylacrylate (CMA) with acrylamide)[23] and in micelle−

(21) (a) Gregor, H. P. In *Polyelectrolytes*; Selegny, E., Ed.; D. Reidel: Dordrecht, 1974; p 87. (b) Struass, U. P.; Leung, Y. P. *J. Am. Chem. Soc.* **1965**, *87*, 1476. (c) Rinaudo, M.; Milas, M. *J. Chim. Phys.* **1969**, *76*, 254. (d) Eldridge, R. J.; Treloar, F. E. *J. Phys. Chem.* **1976**, *80*, 1513.

(22) Kruyt, H. R. *Colloid Science*; Elsevier Publication Company: New York, 1949; Vol. II, pp 335−432.

Table 1. pH_c, α_c, σ_g, σ_{GC}, and $\xi\sigma_{GC}$ for PMAPTAC and Copolymers of MAPTAC and Acrylamide Obtained from Turbidimetric Titration at Various Ionic Strengths

MAPTAC (%)	ξ ($\times 10^8$ cm^{-1})	I	pH_c	α_c	σ_c, ($\times 10^{-4}$ esu/cm^2)	$\sigma_{c,GC}$ ($\times 10^{-4}$ esu/cm^2)	$\sigma_{c,GC}\xi$ ($\times 10^3$ esu/cm^3)
100	0.40	0.30	3.44	0.08	1.1	0.7	3.0
60	0.24	0.10	3.46	0.07	1.0	0.7	1.7
		0.20	3.77	0.10	1.4	1.2	2.9
		0.30	4.24	0.17	2.3	1.8	4.4
		0.40	4.60	0.22	3.0	2.1	5.1
40	0.16	0.10	3.47	0.07	1.0	0.7	1.1
		0.20	4.02	0.15	2.1	1.6	2.6
		0.30	4.52	0.21	2.9	2.0	3.2
		0.40	4.96	0.30	4.1	2.6	4.1
30	0.12	0.10	3.65	0.08	1.1	0.9	1.0
		0.20	4.36	0.19	2.6	2.1	2.5
		0.30	4.93	0.30	4.1	2.6	3.1
15	0.06	0.025	4.30	0.13	1.8	1.29	0.77
		0.050	4.66	0.14	1.9	1.89	1.13
		0.075	4.92	0.23	3.2	2.24	1.34
		0.100	5.25	0.30	4.1	2.65	1.57

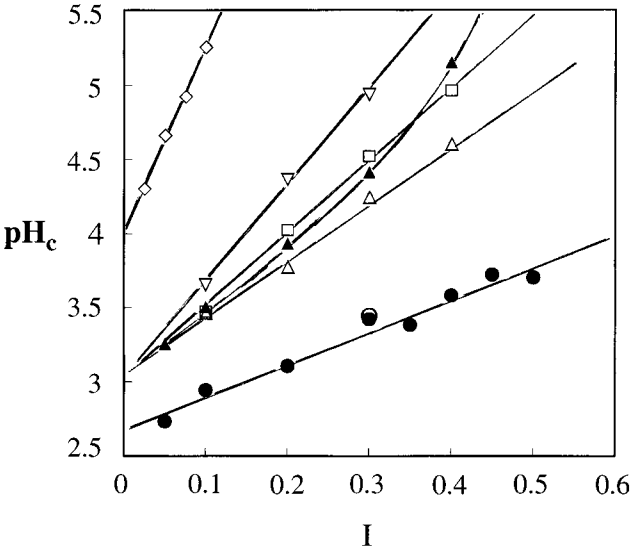

Figure 5. pH_c versus ionic strength in TMACl for PMAPTAC (○), MAPTAC−AAm copolymer (60%/40%) (△), MAPTAC−AAm copolymer (40%/60%) (□), MAPTAC−AAm copolymer (30%/70%) (▽), MAPTAC−AAm copolymer (15%/85%) (◇), MAPTAC−AAm copolymer (60%/40%) in NaCl (▲), and PDADMAC in NaCl (●).

Table 2. pH_c, α_c, σ_g, σ_{GC}, and $\xi\sigma_{GC}$ for PMAPTAC ($\xi = 0.16 \times 10^8$ cm-1) Obtained from Turbidimetric Titration at Various Ionic Strengths

I	pH_c	α_c	σ_g, ($\times 10^{-4}$ esu/cm^2)	$\sigma_{c,GC}$ ($\times 10^{-4}$ esu/cm^2)	$\sigma_{c,GC}$ ($\times 10^{-3}$ esu/cm^2)
0.20	3.10	0.03	0.4	0.2	0.3
0.30	3.42	0.05	0.7	0.3	0.5
0.35	3.38	0.06	0.8	0.4	0.6
0.40	3.58	0.08	1.1	0.5	0.8
0.45	3.72	0.09	1.2	0.5	0.8
0.50	3.7	0.1	1.4	0.5	0.8

polyelectrolyte systems (Triton X-100/sodium dodecyl sulfate with PDADMAC versus PMAPTAC).[24] In both cases, binding of anionic colloids to polycations was stronger for PDADMAC. One explanation may be to consider the polyelectrolyte as a cylinder, whose surface charge density then depends on the side chain length. Since the distances between the backbone and the side chain charge are about 6 Å for PMAPTAC and about 2 Å for PDADMAC, the value 0.008 (electronic charges per Å^{-2}) for the cylinder geometric surface charge density obtained for PDADMAC is considerably larger than the value 0.005 obtained for the CMA−AAm copolymer, whose linear charge density is nearly the same as that of the 50% MAPTAC−AAm copolymer.[23] Consequently, G3 binding is stronger for PDADMAC than for MAPTAC−AAm copolymers.

(23) Park, J. M.; Muhoberac, B. B.; Dubin, P. L.; Xia, J. *Macromolecules* **1992**, *25*, 290.
(24) Zhang, H.; et al. Unpublished.

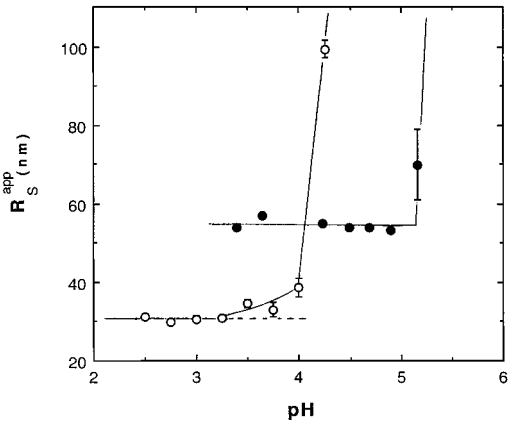

Figure 6. pH dependence of the apparent Stokes−Einstein radius for G3 + PDADMAC in 0.5 M NaCl (○) and G3−PMAPTAC−AAm (15%/85%) in 0.1 M NaCl (●).

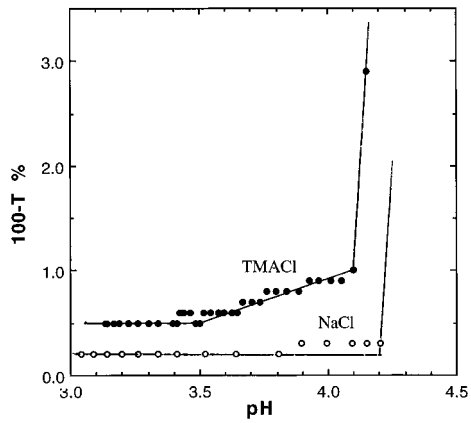

Figure 7. Plots of turbidimetric titration for G3 + PMAPTAC at 0.3 M NaCl (○) and TMACl (●).

Critical Surface Charge Density. The proton dissociation constant K is defined as

$$K_{app} = [COO^-][H^+]/[COOH] = \alpha[H^+]/(1 - \alpha) \quad (7)$$

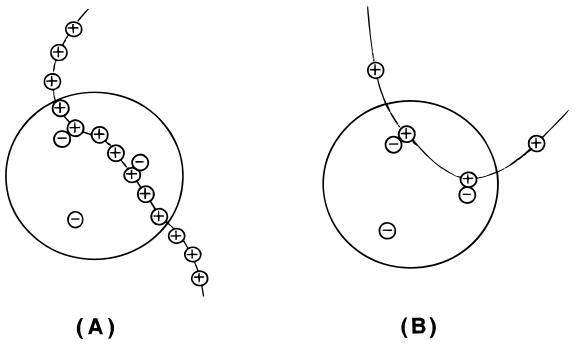

Figure 8. Schematic of complex formation for dendrimer with (a) high charged polyelectrolyte and (b) low charged polyelectrolyte.

If the electrostatic free energy required to dissociate one mole of protons at a given degree of dissociation is $\Delta G_{el}(\alpha)$, then[25]

$$pK_{app} = pK_0 + 0.434\Delta G_{el}(\alpha)/RT \quad (8)$$

where R is the gas constant and K_0 is the characteristic dissociation constant when electrostatic interactions with other dissociated groups are absent. pK_0 is generally obtained as pK_{app} in the limit of $\alpha = 0$. Since $\Delta G_{el}(\alpha)$ is the work of transferring a proton from the bulk solution to the dendrimer surface, then if $eN\psi_0 = \Delta G_{el}(\alpha)$,

$$\psi_0 = 2.303(pK_a - pK_0)kT/e \quad (9)$$

where e is the elementary charge, 4.8×10^{-10} esu, N is Avogadro's number, and ψ_0 is the surface potential (statvolt).

The relationship between ψ_0 and σ_c for spheres is given by the Gouy−Chapman relation:[26]

$$\sigma_{GC} = (\epsilon\psi_0/4\pi)(\kappa + 1/a) \quad (10)$$

where κ is the Debye−Hückel parameter, ϵ is the dielectric constant of the solvent (taken as 78), and a is the dendrimer radius: 1.73 nm at acidic pH.[19−20] The geometric critical surface charge density was also estimated as $\sigma_g = ne\alpha/4\pi a^2$, where $n = 108$.

Results listed in Tables 1 and 2 are also plotted as the absolute value of σ_{GC} against κ in Figure 9. Also included are results for the reverse-charged micelle−polyelectrolyte system, comprised of DMDAO (a cationic micelle with radius 2.6 nm[9]) and PAMPS (an anionic polyelectrolyte with charge spacing nearly the same as that of PMAPTAC). As seen in Figure 9, the dependence of σ_{GC} on κ is linear within the rather wide limits of experimental error, and the slope is an inverse function of polyelectrolyte charge density, as expected from eq 1. In conflict with eq 1, the straight lines determined by the least-squares method do not extrapolate to $\sigma_{GC} = 0$ at $\kappa = 0$. However, since the number of COO^- ions per dendrimer is less than 10 when $\sigma_{GC} < 0.5$, it is difficult to justify a model of a uniformly charged sphere for G3.

The results obtained for six different systems, over a range of ionic strengths, are summarized in Figure 10 as the dependence of $\sigma_{GC}\xi$ on κ. Aside from two aberrant data points, the results for PMAPTAC and MAPTAC copolymers roughly conform to a single curve, with the results for the polyelectrolyte−micelle system forming a parallel curve, shifted toward smaller $\sigma_{GC}\xi$. The large radius of DMDAO micelles relative to that of G3 may be expected to favor polyelectrolyte binding, much as the binding of PDADMAC to G3 is stronger than its binding to G1 at equal σ;[27] this leads to complex formation at lower $\sigma_{GC}\xi$. The values of $\sigma_{GC}\xi$ for PDADMAC are much smaller, possibly reflecting the large geometric charge density of

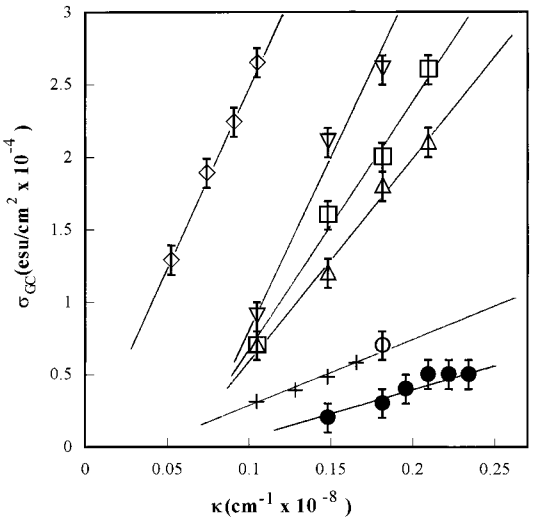

Figure 9. σ_c vs κ in TMACl for: PMAPTAC (○), MAPTAC−AAm copolymer (60%/40%) (△), MAPTAC−AAm copolymer (40%/60%) (□), MAPTAC−AAm copolymer (30/70%) (▽), MAPTAC−AAm copolymer (15%/85%) (◇), MAPTAC−AAm copolymer (60%/40%) in NaCl (▲), and DMDAO−PAMPS in NaCl (+).

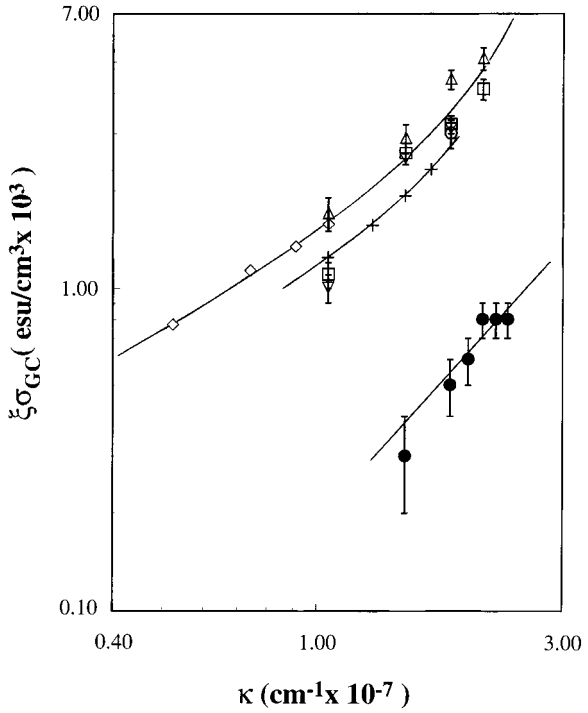

Figure 10. Log−log plots of $\sigma_{GC}\xi$ against κ in TMACl for PMAPTAC (○), MAPTAC−AAm copolymer (60%/40%) (△), MAPTAC−AAm copolymer (40%/60%) (□), MAPTAC−AAm copolymer (30%/70%) (▽), MAPTAC−AAm copolymer (15%/85%) (?), and DMDAO−PAMPS in NaCl (●).

(25) Morawetz, H. *Macromolecules in Solution*, 2nd ed.; John Wiley & Sons: New York, 1975; pp 344−396.

(26) Loeb, A. L.; Overbeek, J. Th. G.; Wiersema, P. H. *The Electrical Double Layer around a Spherical Particle*; MIT Press: Cambridge, U.K., 1961.

(27) Zhang, H.; Ray, J.; Manning, G. S.; Moorefield, C.; Newkome, G.; Dubin, P. L. *J. Phys. Chem.*, in press.

PDADMAC (see above). However, most of the data obtained for G3 in the range $\kappa = 0.5 \times 10^7$ to 1.7×10^7 ($0.025 < I < 0.25$) when presented on a log−log plot approximate a straight line with slope 1.1 ± 0.1, corresponding to $\sigma_{GC}\xi = (\text{constant})\kappa^{1.1}$, in close agreement with eq 1. This is also quite close to the $\kappa^{1.2}$ dependence of σ_{GC} arising from the model of Muthukumar[5] in the range of low κ.[17]

The considerable scatter among the combined data in Figure 10 may result from several sources. First, we assume that the copolymers have homogeneous charge distributions. The copolymer sequence distribution could, in principle, lead to MAPTAC-rich domains of the polycation which preferentially bind to G3. Second, in parametrizing the polymers solely according to average charge spacing, we neglect the effects of polymer composition on chain stiffness, which has been shown to have a large influence on σ_{GC}.[17] This effect should become particularly important for small colloid particles such as G3, where complexation may involve substantial local deformation of the polymer chain.[27]

Conclusions

Electrostatic interactions between dendrimer G3 and polyelectrolytes of varying charge density (ξ) confirm the occurrence of complex formation as a phase-transition-like phenomenon. The critical condition σ_{GC} depends on ξ and κ and, in TMACl, is expressed by $\sigma_{GC}\xi \sim \kappa^{1.1}$ in the range $0.025 < I < 0.25$. Na^+ impedes the complexation by counterion binding. The difference of σ_{GC} between PDADMAC and the MAPTAC−AAm copolymer suggests consideration of polyelectrolyte charge density according to a cylindrical model. When highly charged polyelectrolytes such as PDADMAC bind to G3 at small σ_{GC}, soluble complexes may appear because charge asymmetry precludes stoichiometric charge neutralization.

Acknowledgment. This work was supported by NSF Grant DMR 9619772 and Petroleum Research Fund Grant PRF32625-AC7, administered by the American Chemical Society, (P.L.D.) and NSF Grant DMR 9622609 (G.R.N.).

LA990125L